## Supporting Information

# Trimethylsilyl Group-Assisted Stimuli-Response: Self-Assembly of 1,3,6,8-Tetra(trimethysilylethynyl)pyrene

Feng Xu,[a] Takanori Nishida,[a] Kenta Shinohara,[a] Lifen Peng,[a] Makoto Takezaki,[a] Takahiro Kamada,[b] Haruo Akashi,[b] Hiromu Nakamura,[c] Kouki Sugiyama,[c] Kazuchika Ohta,[c] Akihiro Orita*[a] and Junzo Otera[a]

[a]Department of Applied Chemistry and Biotechnology, Okayama University of Science, 1-1 Ridai-cho, Kita-ku, Okayama 700 0005 Japan, [b]Research Institute of Natural Sciences, Okayama University of Science, 1-1 Ridai-cho, Kita-ku, Okayama 700 0005 Japan, [c]Smart Material Science and Technology, Interdisciplinary Graduate School of Science and Technology, Shinshu University 1-15-1 Tokida, Ueda, 386 8567 Japan

**Table of contents**

1. General consideration S4
2. Structure of **Y-form** S4
**Figure S1**. ORTEP diagram of **Y-form** S4
**Figure S2**. Packing structures of **Y-form** S5
**Table S1**. Crystal data and structure refinements for **Y-form** S6
3. XRD profiles of $\mathbf{O_C}$-, $\mathbf{O_A}$- and $\mathbf{O_K}$-**forms** S10
**Figure S3**. XRD profile of **Oc-form** S10
**Table S2**. X-ray diffraction data of $\mathbf{O_C}$-**form** S10
**Figure S4**. Lattice constants [Å] of $\mathbf{O_C}$-**form** S11
**Figure S5**. XRD profile of $\mathbf{O_A}$-**form** S11
**Figure S6**. XRD profile of $\mathbf{O_K}$-**form** S12
**Table S3**. X-ray diffraction data of $\mathbf{O_K}$-**form** S12
**Figure S7**. Lattice constants [Å] of $\mathbf{O_K}$-**form** S13
4. Recrystallization/reprecipitation of **1** S14
**Table S4**. Conditions and results in recrystallization/reprecipitation of **1** S14
**Figure S8**. PL spectra of **Y-forms** and $\mathbf{O_C}$-**forms** obtained from recrystallization/reprecipitaion S14
5. DSC measurements of **1** S15
**Figure S9**. DSC profiles of **Y-form** S15
**Figure S10**. DSC profiles of $\mathbf{O_A}$-**form** S16
6. Thermochromism of **1** S17
**Scheme S1**. Summary of thermochromism of **1** S17
6.1 Thermal phase transition of **Y-form** to $\mathbf{O_C}$-**form** S17

**Figure S11**. Pictures of **Y-** and **$O_C$-forms** in thermochromic phase transition S17
**Figure S12**. PL spectrum of **$O_C$-form** which was obtained by heating **Y-form** S17
6.2 Thermal phase transition of **$O_A$-form** to **$O_K$-form** S18
**Figure S13**. Pictures of **$O_C$-**, **$O_K$-** and **$O_A$-forms** under sunlight and UV-light S18
**Figure S14**. PL profiles of **$O_C$-, $O_K$-** and **$O_A$-forms** S18
7. Vapochromism S19
**Scheme S2**. Summary of vapochromism of **1** S19
7.1 Acetone-promoted phase transition of **$O_C$-, $O_A$-** and **$O_K$-forms** to **Y-form** S19
**Figure S15**. Apparatus for vapochromic phase transition S19
**Figure S16**. PL profiles of **Y-forms** which were obtained by vapochromic phase transition from **$O_C$-**, **$O_A$-** and **$O_K$-forms** S20
7. 1.1 Vapochromic phase transition from **$O_C$-form** to **Y-form** S21
**Figure S17**. Pictures of **$O_C$-** and **Y-forms** in acetone-promoted vapochromism S21
**Figure S18**. DSC profiles of **Y-form** obtained from **$O_C$-form** by acetone-promoted phase transition S21
7. 1.2 Vapochromic phase transition from **$O_A$-form** to **Y-form** S22
**Figure S19**. Pictures of **$O_A$-** and **Y-forms** in acetone-promoted vapochromism S22
**Figure S20**. DSC profiles of **Y-form** obtained from **$O_A$-form** by acetone-promoted phase transition S22
7. 1.3 Vapochromic phase transition from **$O_K$-form** to **Y-form** S23
**Figure S21**. Pictures of **$O_K$-** and **Y-forms** in acetone-promoted vapochromism S23
**Figure S22**. DSC profiles of **Y-form** obtained from **$O_K$-form** by acetone-promoted phase transition S23
7.2 Hexane-promoted phase transition of **$O_A$-** and **$O_K$-forms** to **$O_C$-form** S24
**Figure S23**. PL spectra of authentic **$O_C$-form** and **$O_C$-form** obtained from **$O_A$-form** S24
**Figure S24**. PL spectra of authentic **$O_C$-form** and **$O_C$-form** obtained from **$O_K$-form** S25
**Figure S25**. PL spectra of authentic **Y-form** and **Y-form** exposed to hexane vapor S25
8. Mechanochromism of **1** S26
**Scheme S3**. Summary of mechanochromism of **1** S26
**Figure S26**. Pictures of **Y-** and **$O_A$-forms** in grinding-promoted mechanochromism S26
**Figure S27**. PL spectra of **$O_A$-forms** which were obtained by mechanochromic phase transition from **Y-**, **$O_C$-** and **$O_K$-forms** S27
9. Fluorescence life time S28
**Figure S28**. Fluorescence decay profiles of **1** S28
**Table S5**. Summary of emission lifetime, PL quantum yield and rate constants S29
10. Thermogravimetry analysis (TGA) S30
**Figure S29**. TGA thermogram of **$O_C$-form** S30
11. UV—Vis absorption and PL spectra of **1** in $CH_2Cl_2$ S30
**Figure S30**. UV—Vis absorption spectra of **1** in $CH_2Cl_2$ ($10^{-4}$ to $10^{-5}$ mol/L) S30
**Figure S31**. PL spectra of **1** in $CH_2Cl_2$ ($10^{-2}$ to $10^{-5}$ mol/L) S31
12. Microscopic observations of **$O_C$-form** on heating S31

**Figure S32**. Microscopic observations of **$O_C$-form** on heating S31
13. XRD analyses and microscopic observations of **$O_K$-form** on heating S32
**Figure S33**. XRD profiles of **$O_K$-form** on heating S32
**Figure S34**. Microscopic observations of **$O_K$-form** on heating S33
14. References of Supporting Information and NMR charts of **1** S34
**Figure S35**. NMR charts of **1** ($CDCl_3$) S35

**1. General Considerations**: Unless otherwise stated, all reactions were carried out under an argon atmosphere. Anhydrous tetrahydrofuran (THF) was purchased and used without further purification. Toluene and i-$Pr_2NH$ were distilled from $CaH_2$ prior to use. All NMR spectra were recorded at ambient temperature (ca. 20 °C) on JEOL LAMBDA 300 and LAMBDA 500 and ECS-400 NMR spectrometers, and referenced to an internal standard tetramethylsilane. MALDI-TOF MS was recorded on BRUKER autoflex speed. UV-vis absorption and emission spectra were measured in degassed solvents at 25 °C. Absolute photoluminescence quantum yield was measured by integrated sphere system. The phase transition sequences for **1** were revealed by using a polarizing optical microscope (Nikon ECLIPSE E600 POL) equipped with a heating plate (Mettler FP82HT hot stage, Mettler FP-90 Central Processor) and a differential scanning calorimeter (Shimadzu DSC-50). The decomposition temperatures were measured by a Rigaku Thermo plus TG 820 thermogravity analyser. The identification of the mesophases was performed by using a small angle X-ray diffractometer (Bruker Mac SAXS System: Cu-Kα radiation) equipped with a heating plate (Mettler FP82HT hot stage, Mettler FP-90 Central Processor).

Compound **1** was prepared according to the reported procedure.[S1] **Y-** and **$O_C$-forms** were obtained by recrystallization from acetone and reprecipitation from hexane, respectively. **$O_A$-form** was obtained by grinding **Y-** or **$O_C$-form** by mortar and pestle. **$O_K$-form** was obtained by heating **$O_A$-form** at 150 °C for 2 h.

**2. Structure of Y-form**

**Figure S1.** ORTEP diagram of **Y-form**

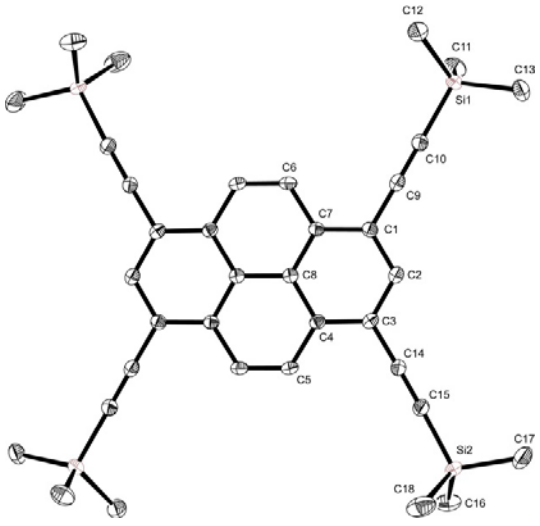


The crystallographically independent atoms are labeled.

Formula: C36 H42 Si4
Unit Cell Parameters: a 6.3160(18) b 10.023(3) c 15.378(5) P-1

CCDC 1490712

**Figure S2.** Packing structures of **Y-form**

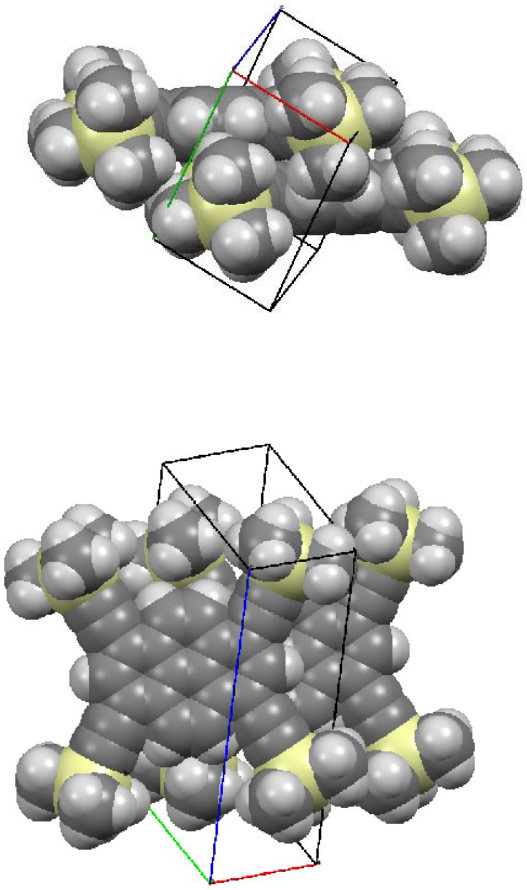

**Table S1.** Crystal data and structure refinements for **Y-form**

A. Crystal Data

| | |
|---|---|
| Empirical Formula | $C_{36}H_{42}Si_4$ |
| Formula Weight | 587.07 |
| Crystal Color, Habit | yellow, platelet |
| Crystal Dimensions | 0.450 X 0.060 X 0.010 mm |
| Crystal System | triclinic |
| Lattice Type | Primitive |
| Lattice Parameters | a = 6.316(2) Å<br>b = 10.023(3) Å<br>c = 15.378(5) Å<br>$\alpha$ = 70.431(9) $^o$<br>$\beta$ = 81.290(12) $^o$<br>$\gamma$ = 80.513(13) $^o$<br>V = 899.9(5) Å$^3$ |
| Space Group | P-1 (#2) |
| Z value | 1 |
| $D_{calc}$ | 1.083 g/cm$^3$ |
| $F_{000}$ | 314.00 |
| $\mu$(MoK$\alpha$) | 1.865 cm$^{-1}$ |

B. Intensity Measurements

| | |
|---|---|
| Diffractometer | Saturn724 |
| Radiation | MoKα (λ = 0.71075 Å)<br>multi-layer mirror monochromated |
| Voltage, Current | 50kV, 24mA |
| Temperature | -179.8°C |
| Detector Aperture | 70 x 70 mm |
| Data Images | 2520 exposures |
| ω oscillation Range | -110.0 - 70.0° |
| Exposure Rate | 8.0 sec./° |
| Detector Swing Angle | -19.51° |
| ω oscillation Range | -110.0 - 70.0° |
| Exposure Rate | 8.0 sec./° |
| Detector Swing Angle | -19.51° |
| ω oscillation Range | -110.0 - 70.0° |
| Exposure Rate | 8.0 sec./° |
| Detector Swing Angle | -19.51° |
| ω oscillation Range | -110.0 - 70.0° |
| Exposure Rate | 8.0 sec./° |
| Detector Swing Angle | -19.51° |

| | |
|---|---|
| ω oscillation Range | -110.0 - 70.0° |
| Exposure Rate | 8.0 sec./° |
| Detector Swing Angle | -19.51° |
| ω oscillation Range | -110.0 - 55.0° |
| Exposure Rate | 8.0 sec./° |
| Detector Swing Angle | -19.51° |
| ω oscillation Range | -76.0 - 59.0° |
| Exposure Rate | 8.0 sec./° |
| Detector Swing Angle | -19.51° |
| ω oscillation Range | -110.0 - -50.0° |
| Exposure Rate | 8.0 sec./° |
| Detector Swing Angle | -19.51° |
| Detector Position | 45.04 mm |
| Pixel Size | 0.141 mm |
| $2\theta_{max}$ | 60.1° |
| No. of Reflections Measured | Total: 24975<br>Unique: 4111 ($R_{int}$ = 0.0476) |
| Corrections | Lorentz-polarization<br>Absorption<br>(trans. factors: 0.887 - 0.998) |

C. Structure Solution and Refinement

| | |
|---|---|
| Structure Solution | Direct Methods |
| Refinement | Full-matrix least-squares on $F^2$ |
| Function Minimized | $\Sigma$ w ($Fo^2$ - $Fc^2$)$^2$ |
| Least Squares Weights | w = 1/ [ $\sigma^2(Fo^2)$ + (0.0394 · P)$^2$ + 0.9802 · P ]<br>where P = (Max($Fo^2$,0) + 2$Fc^2$)/3 |
| $2\theta_{max}$ cutoff | 55.0$^o$ |
| Anomalous Dispersion | All non-hydrogen atoms |
| No. Observations (All reflections) | 4111 |
| No. Variables | 181 |
| Reflection/Parameter Ratio | 22.71 |
| Residuals: R1 (I>2.00$\sigma$(I)) | 0.0545 |
| Residuals: R (All reflections) | 0.0621 |
| Residuals: wR2 (All reflections) | 0.1218 |
| Goodness of Fit Indicator | 1.098 |
| Max Shift/Error in Final Cycle | 0.001 |
| Maximum peak in Final Diff. Map | 0.45 $e^-$/Å$^3$ |
| Minimum peak in Final Diff. Map | -0.25 $e^-$/Å$^3$ |

### 3. XRD profiles of $O_C$-, $O_A$- and $O_K$-forms

**Figure S3.** XRD profile of **Oc-form**

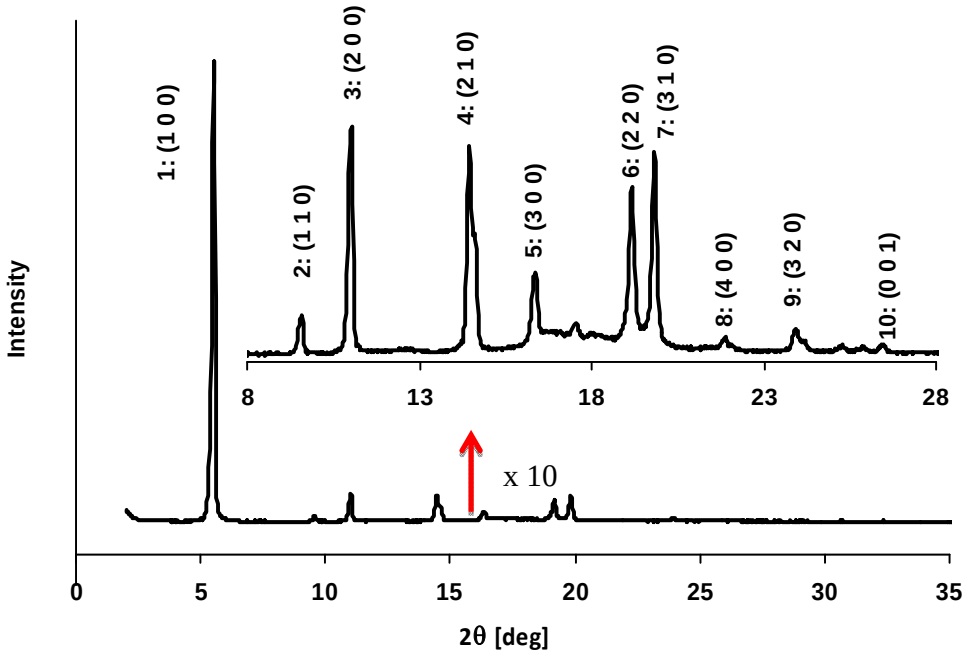


**Table S2.** X-ray diffraction data of **$O_C$-form**

| Peak no. | Spacing | | | Miller indices (*h k l*) |
|---|---|---|---|---|
| | 2θ [deg] | Obsd [Å] | calcd [Å] | |
| 1 | 5.52 | 16.0 | 16.0 | (1 0 0) |
| 2 | 9.59 | 9.21 | 9.26 | (1 1 0) |
| 3 | 11.02 | 8.20 | 8.02 | (2 0 0) |
| 4 | 14.46 | 6.12 | 6.06 | (2 1 0) |
| 5 | 16.37 | 5.41 | 5.35 | (3 0 0) |
| 6 | 19.17 | 4.63 | 4.63 | (2 2 0) |
| 7 | 19.82 | 4.47 | 4.45 | (3 1 0) |
| 8 | 21.88 | 4.08 | 4.01 | (4 0 0) |
| 9 | 23.92 | 3.72 | 3.68 | (3 2 0) |
| 10 | 26.45 | 3.37 | -- | (0 0 1) |

**Figure S4.** Lattice constants [Å] of **$O_C$-form**

| *a* | *h* | *Z* |
|---|---|---|
| **18.5** | **3.37** | **1.0 for ($\rho$ = 1.0)** |

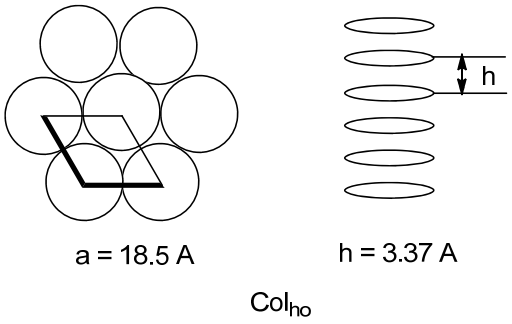


**Figure S5.** XRD profile of **$O_A$-form**

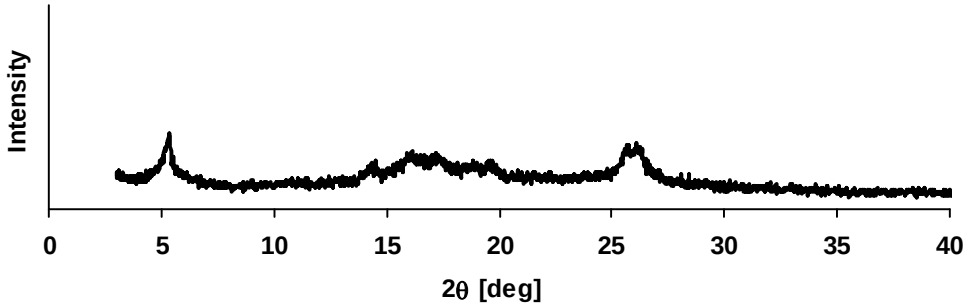

**Figure S6.** XRD profile of **$O_K$-form**

**$O_K$-form** was prepared by heating **$O_A$-form** at 265 °C and subjected to XRD analysis.

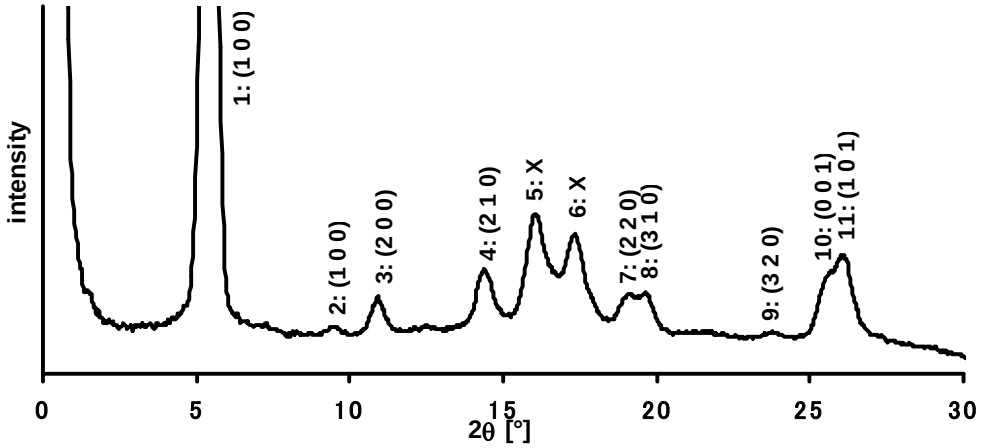


**Table S3.** X-ray diffraction data of **$O_K$-form**

| Peak no. | Spacing | | | Miller indices (*h k l*) |
|---|---|---|---|---|
| | 2θ [deg] | Obsd [Å] | calcd [Å] | |
| 1 | 5.42 | 16.34 | 16.31 | (1 0 0) |
| 2 | 9.50 | 9.35 | 9.42 | (1 1 0) |
| 3 | 10.92 | 8.11 | 8.16 | (2 0 0) |
| 4 | 14.36 | 6.16 | 6.16 | (2 1 0) |
| 5 | 16.06 | 5.51 | --- | X |
| 6 | 17.34 | 5.11 | --- | X |
| 7 | 19.14 | 4.65 | 4.71 | (2 2 0) |
| 8 | 19.64 | 4.52 | 4.52 | (3 1 0) |
| 9 | 23.74 | 3.74 | 3.74 | (3 2 0) |
| 10 | 25.70 | 3.47 | --- | (0 0 1) |
| 11 | 26.06 | 3.42 | --- | (1 0 1) |

$$\frac{1}{d_{101}^2} = \frac{1^2}{a^2} + \frac{1^2}{c^2}$$ , (a = 18.8 Å, c = 3.47 Å)

$d_{101}$ = 3.39 Å (calcd), 3.42 Å (observed)

**Figure S7.** Lattice constants [Å] of **$O_K$-form**

| ***a*** | ***h*** | ***Z*** |
|---|---|---|
| **18.8** | **3.47** | **1.1 for ($\rho$ = 1.0)** |

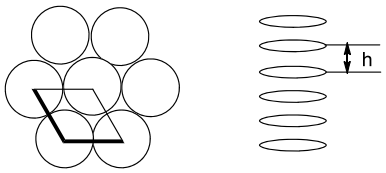


plastic $Col_{ho}$

## 4. Recrystallization/reprecipitation of 1

**Table S4.** Conditions and results in recrystallization/reprecipitation of **1**

| Solvent used for recrystallization/reprecipitation | Form |
|---|---|
| Acetone[a] | **Y-form** |
| ethyl acetate[a] | **Y-form** |
| $CH_2Cl_2/CH_3CN$[c] | **Y-form** |
| $CHCl_3$[b] | **$O_C$-form** |
| 1,2-dichloroethane[b] | **$O_C$-form** |
| Hexane[a] | **$O_C$-form** |
| Heptane[a] | **$O_C$-form** |
| c-hexane[a] | **$O_C$-form** |
| Benzene[b] | **$O_C$-form** |
| $Et_2O$[b] | **$O_C$-form** |
| THF[b] | **$O_C$-form** |
| [a]Saturated solution was kept in a sealed flask at room temperature. [b]Saturated solution was kept at room temperature, and the solvent was gradually evaporated. [c]A small amount of $CH_3CN$ was added to a saturated $CH_2Cl_2$ solution. | |

**Figure S8.** PL spectra of **Y-forms** and **$O_C$-forms** obtained from recrystallization/reprecipitation

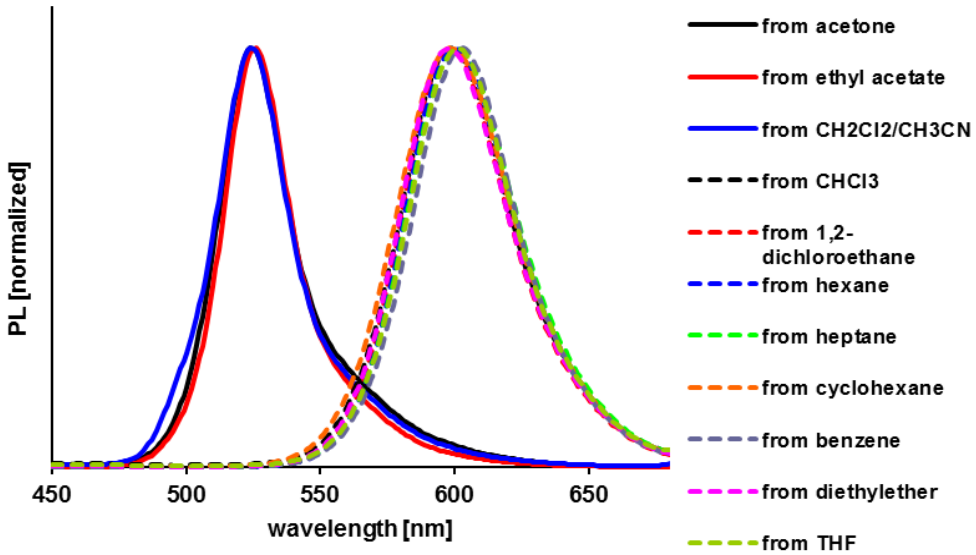

**5. DSC measurements of 1**

DSC thermograms were recorded using the virgin samples of **1** at 10 °C/min on heating and -10 °C/min on cooling rates.

**Figure S9.** DSC profiles of **Y-form**

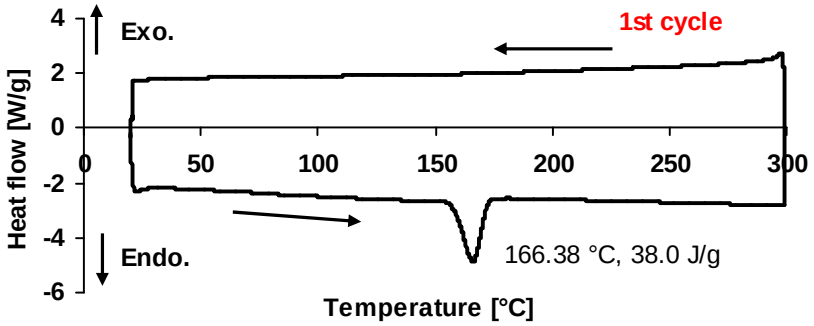


At 166 °C in the first cycle, **Y-form** underwent the phase transition to **$O_C$-from**.

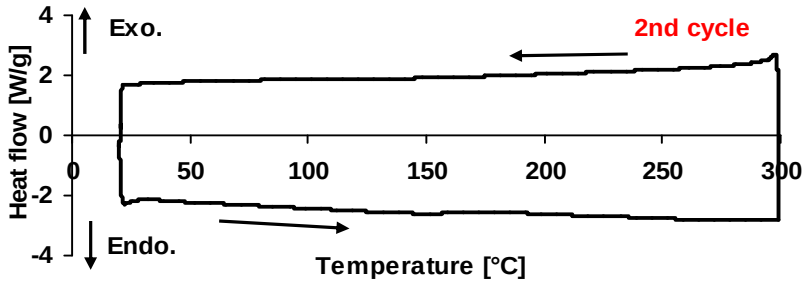


In the second cycle, neither exothermic nor endothermic profile was recorded diagnostic of no phase transition of **$O_C$-form**.

**Figure S10.** DSC profiles of **$O_A$-form**

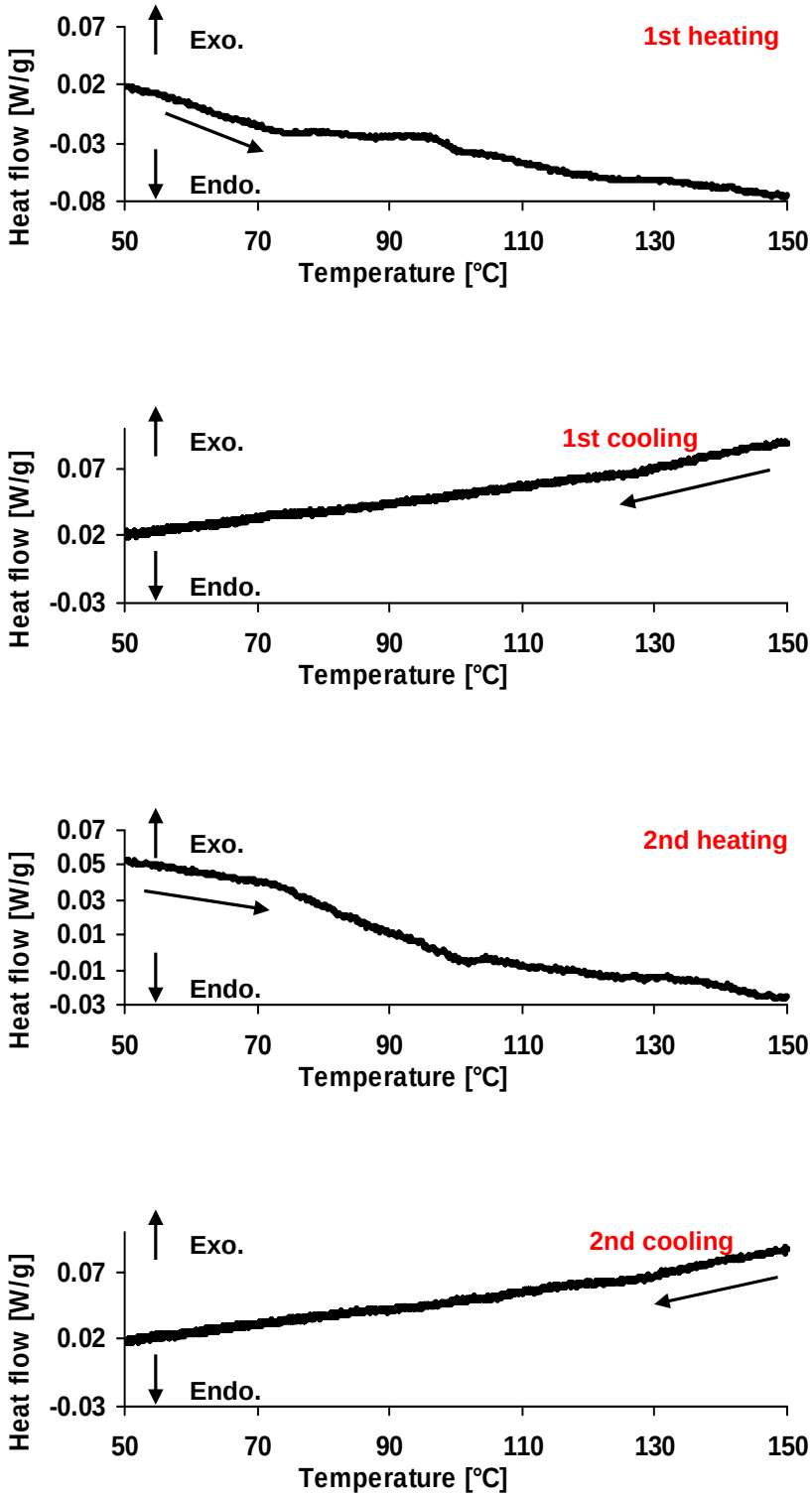

## 6. Thermochromism of 1

**Scheme S1.** Summary of thermochromism of **1**

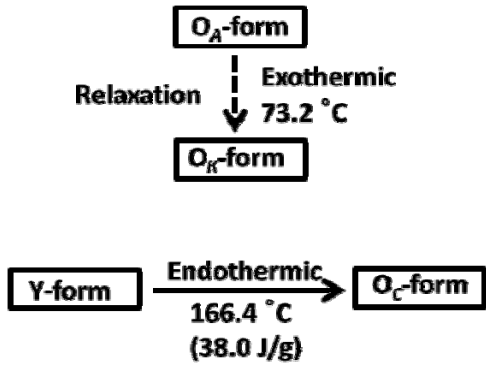


### 6.1 Thermal phase transition of Y-form to $O_C$-form

**Y-form 1** was placed on a thin glass plate and heated by a hot plate until the color changed to orange (~250 °C). Phase transitions were confirmed by color and PL profile.

**Figure S11.** Pictures of **Y-** and **$O_C$-forms** in thermochromic phase transition

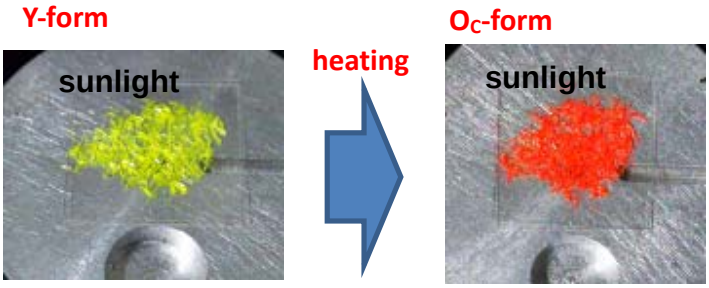


**Figure S12.** PL spectrum of **$O_C$-form** which was obtained by heating **Y-form**

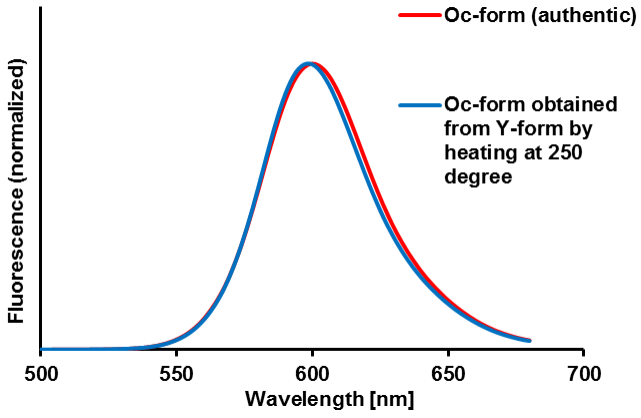

### 6.2 Thermal phase transition of $O_A$-form to $O_K$-form

**$O_A$-form** was placed on a thin glass plate and heated by a hot plate at 270 °C for 12 h. Phase transition was confirmed by comparison of PL profiles because **O-forms** showed similar orange colors.

**Figure S13.** Pictures of **$O_C$-**, **$O_K$-** and **$O_A$-forms** under sunlight and UV-light

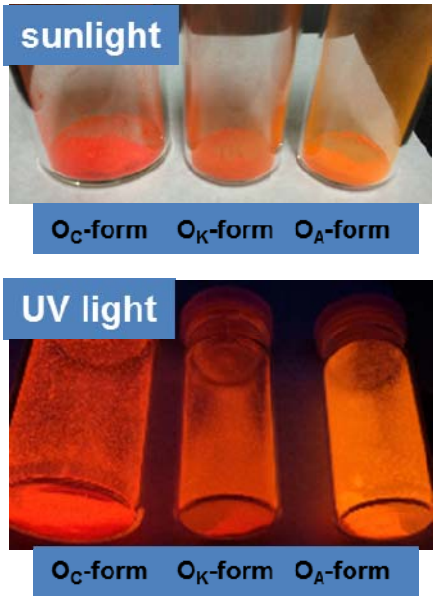


**Figure S14.** PL profiles of **$O_C$-, $O_K$-** and **$O_A$-forms**

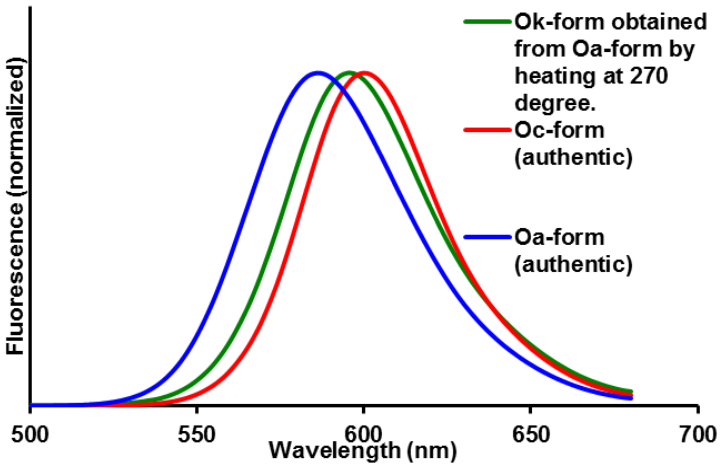

## 7. Vapochromism of 1

**Scheme S2.** Summary of vapochromism of **1**

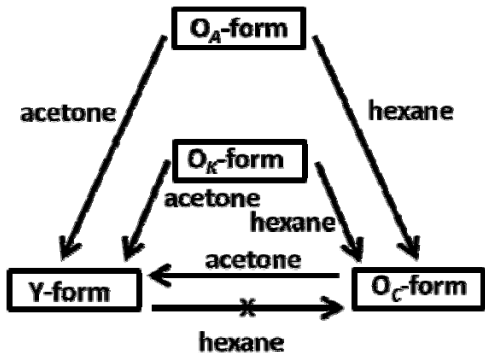


### 7.1 Acetone-promoted phase transition of $O_C$-, $O_A$- and $O_K$-forms to Y-form

In a glass beaker was placed **$O_C$-, $O_A$-** or **$O_K$-form**, and a small amount of acetone was added. The beaker was put a lid on by aluminum foil, and kept at rt overnight. Phase transitions were confirmed by color, PL profiles and DSC.

**Figure S15.** Apparatus for vapochromic phase transition

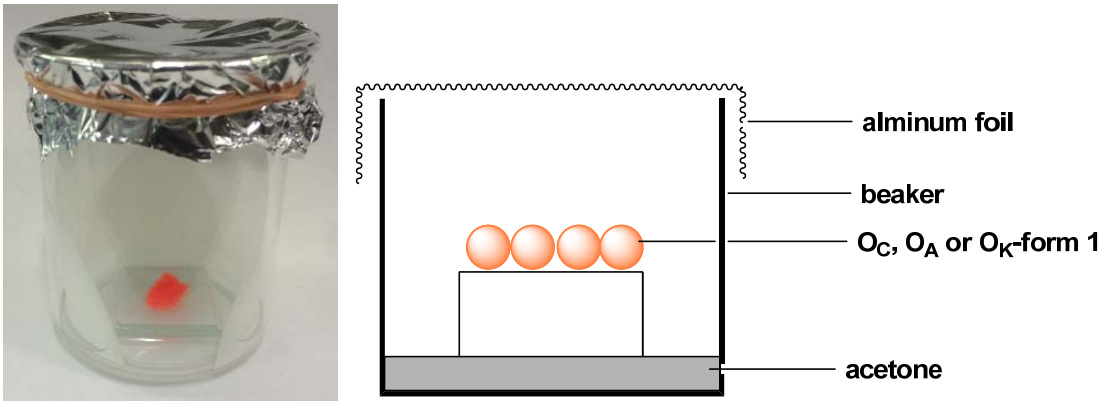

**Figure S16.** PL profiles of **Y-forms** which were obtained by vapochromic phase transition from **$O_C$-**, **$O_A$-** and **$O_K$-forms**.

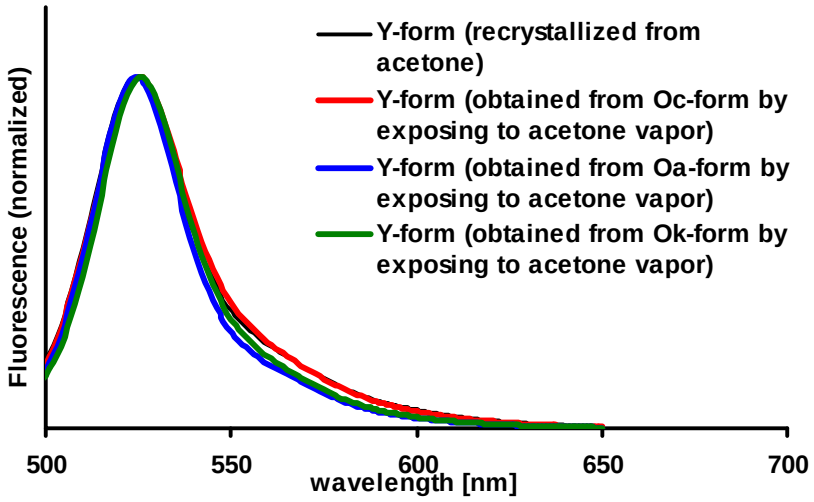

**7. 1.1** Vapochromic phase transition from **$O_C$-form** to **Y-form**

**Figure S17.** Pictures of **$O_C$-** and **Y-forms** in acetone-promoted vapochromism

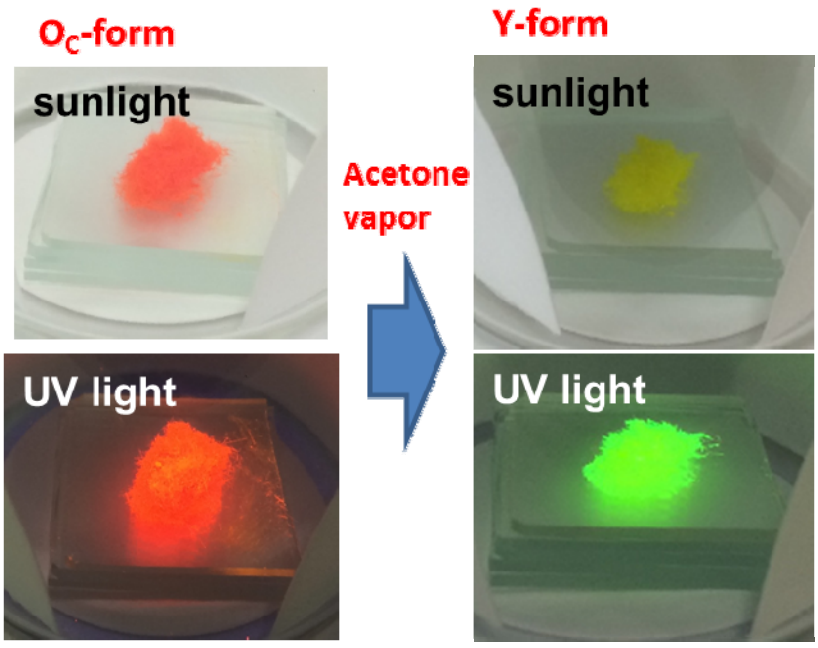


**Figure S18.** DSC profiles of **Y-form** obtained from **$O_C$-form** by acetone-promoted phase transition

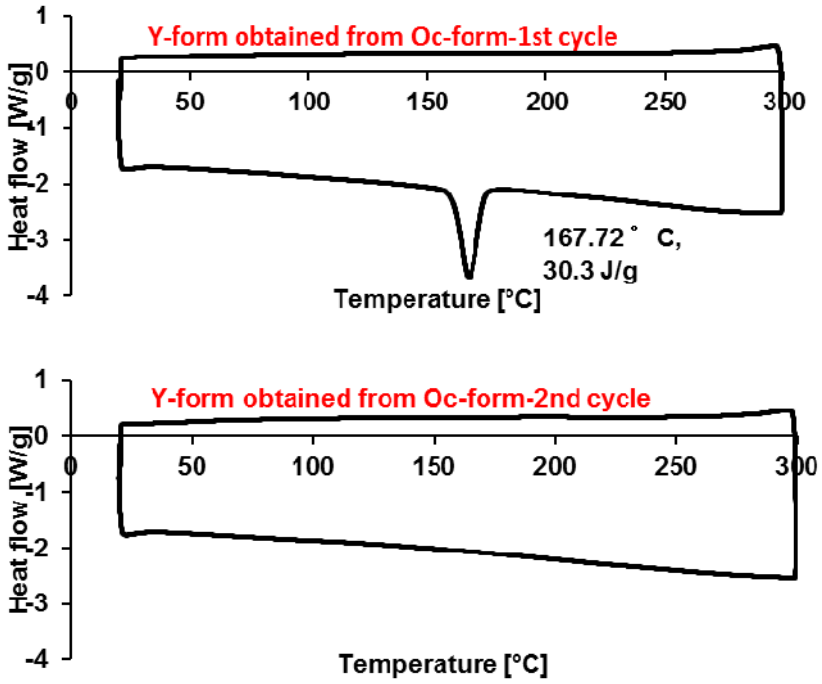

**7. 1.2** Vapochromic phase transition from **$O_A$-form** to **Y-form**

**Figure S19.** Pictures of **$O_A$-** and **Y-forms** in acetone-promoted vapochromism

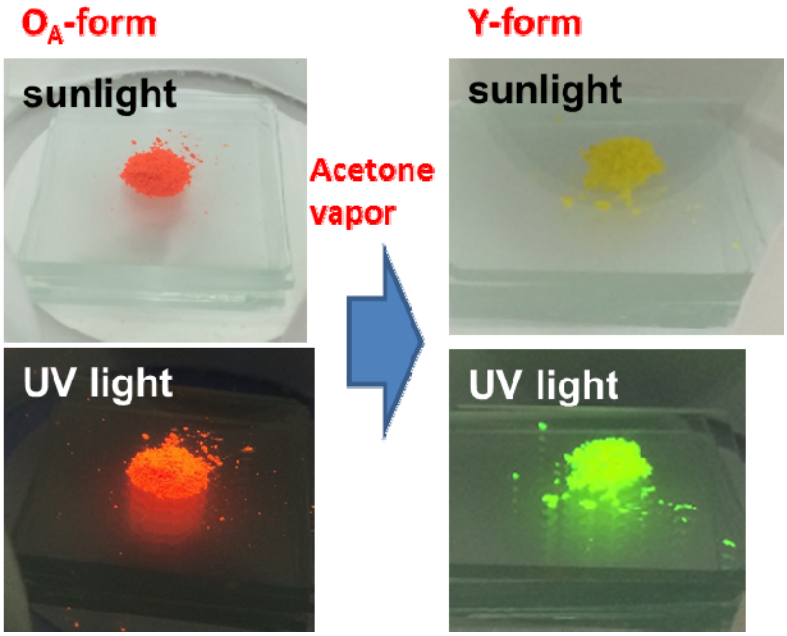


**Figure S20.** DSC profiles of **Y-form** obtained from **$O_A$-form** by acetone-promoted phase transition

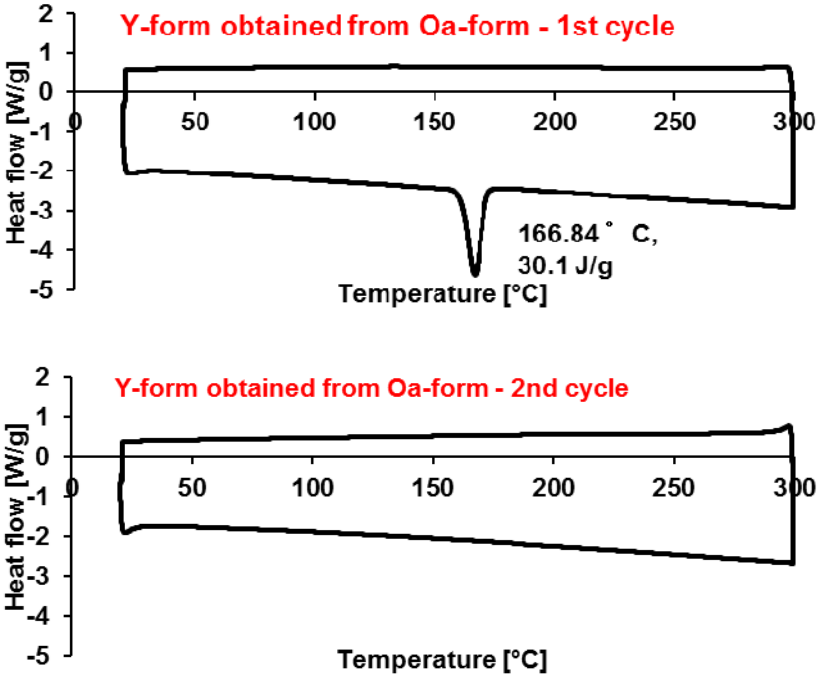

**7. 1.3** Vapochromic phase transition from **$O_K$-form** to **Y-form**

**Figure S21.** Pictures of **$O_K$-** and **Y-forms** in acetone-promoted vapochromism

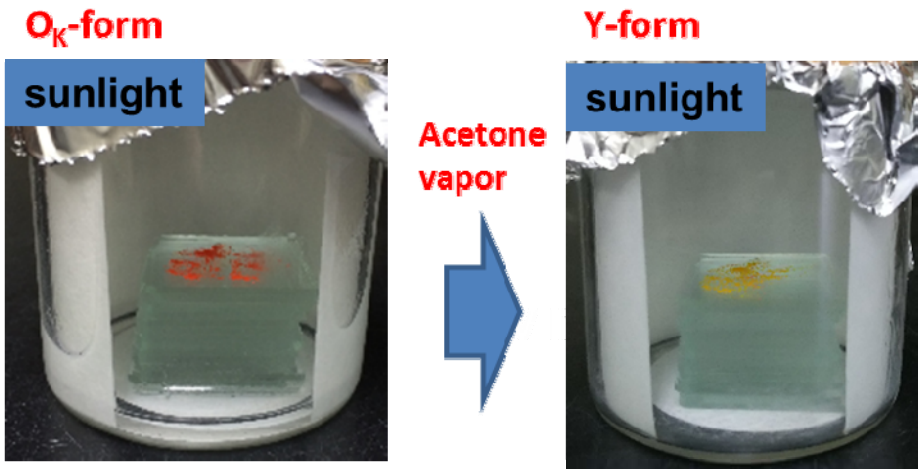


**Figure S22.** DSC profiles of **Y-form** obtained from **$O_K$-form** by acetone-promoted phase transition

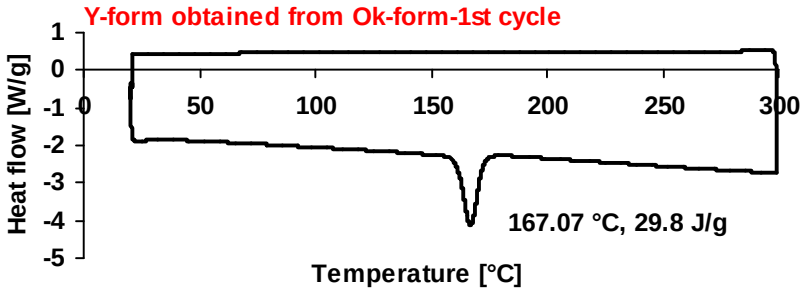


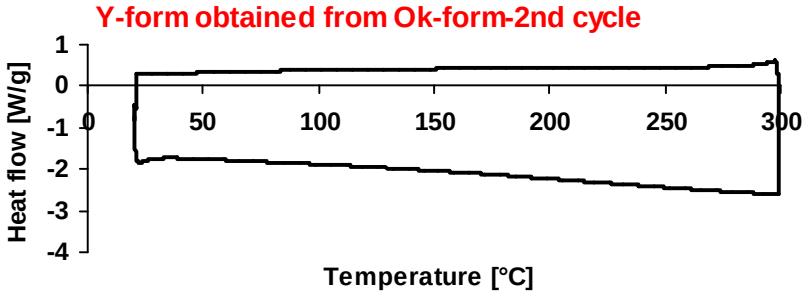

### 7.2 Hexane-promoted phase transition of $O_A$- and $O_K$-forms to $O_C$-form

In a glass beaker was placed **$O_A$-** or **$O_K$-form**, and a small amount of hexane was added. The beaker was put a lid on by aluminum foil, and kept at rt overnight. Phase conversions were confirmed by comparison of PL profiles.

**Figure S23.** PL spectra of authentic **$O_C$-form** and **$O_C$-form** obtained from **$O_A$-form**

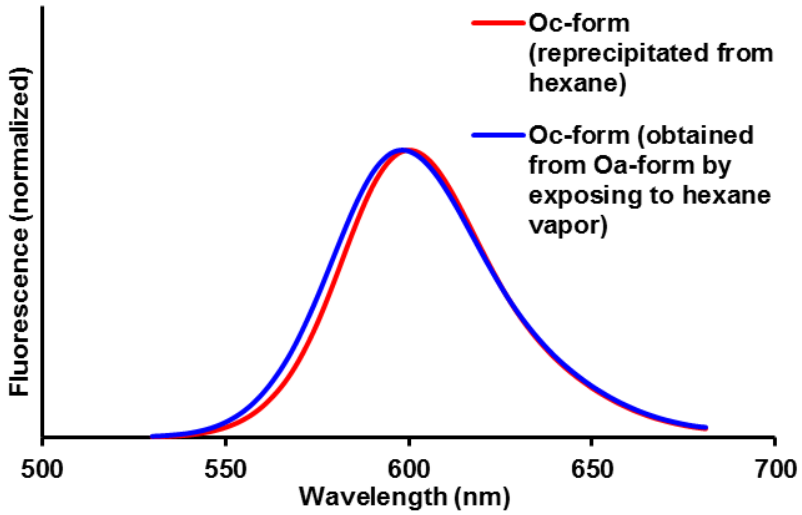

**Figure S24.** PL spectra of authentic **$O_C$-form** and **$O_C$-form** obtained from **$O_K$-form**

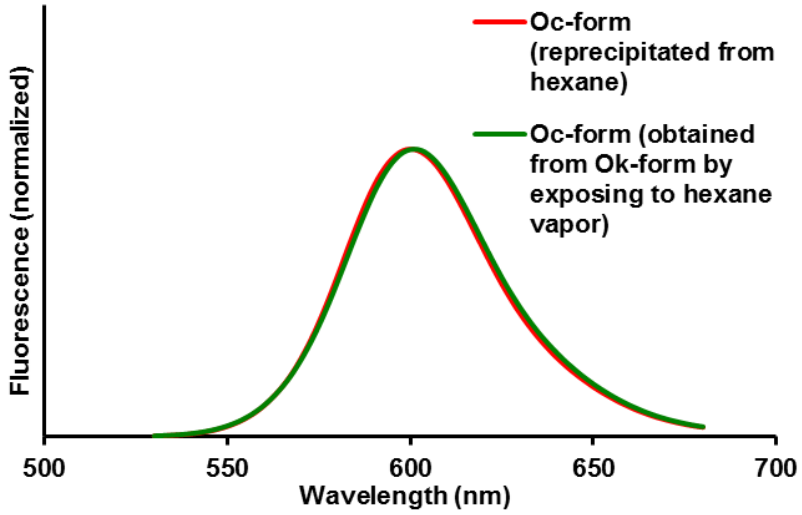


**Figure S25.** PL spectra of authentic **Y-form** and **Y-form** exposed to hexane vapor

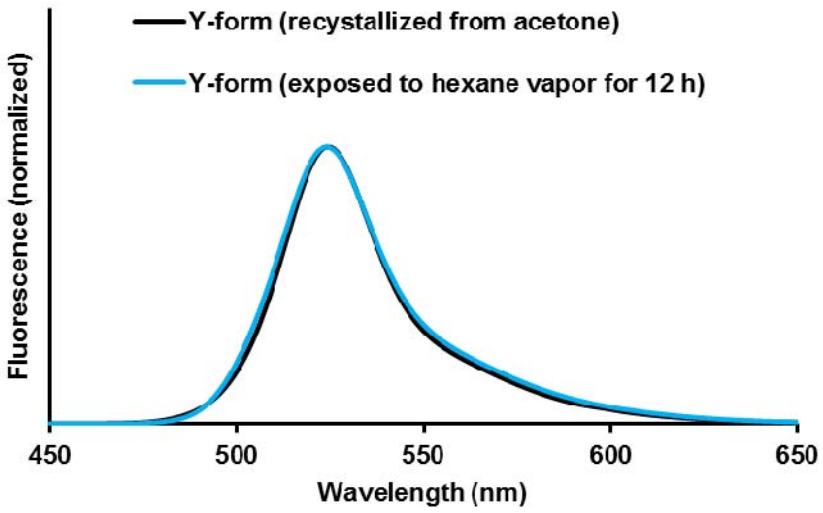


When **Y-form** was exposed to hexane vapor, no color change was observed.

## 8. Mechanochromism of 1

**Scheme S3.** Summary of mechanochromism of **1**

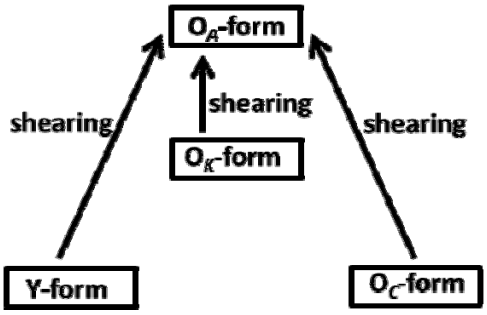


On a mortar was placed **Y-, $O_C$-** or **$O_K$-form 1**, and **1** was ground by a pestle. Phase transitions were confirmed by color change and comparison of PL profiles.

**Figure S26.** Pictures of **Y-** and **$O_A$-forms** in grinding-promoted mechanochromism

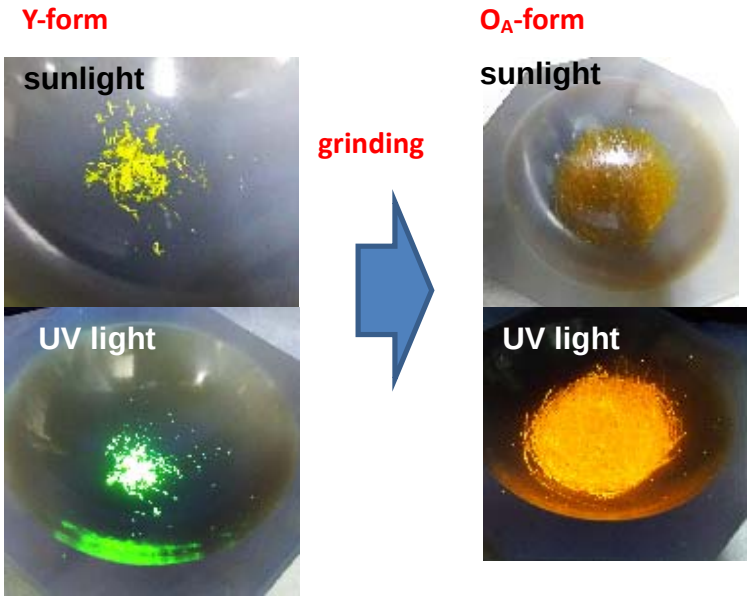

**Figure S27.** PL spectra of **$O_A$-forms** which were obtained by mechanochromic phase transition from **Y-**, **$O_C$-** and **$O_K$-forms**

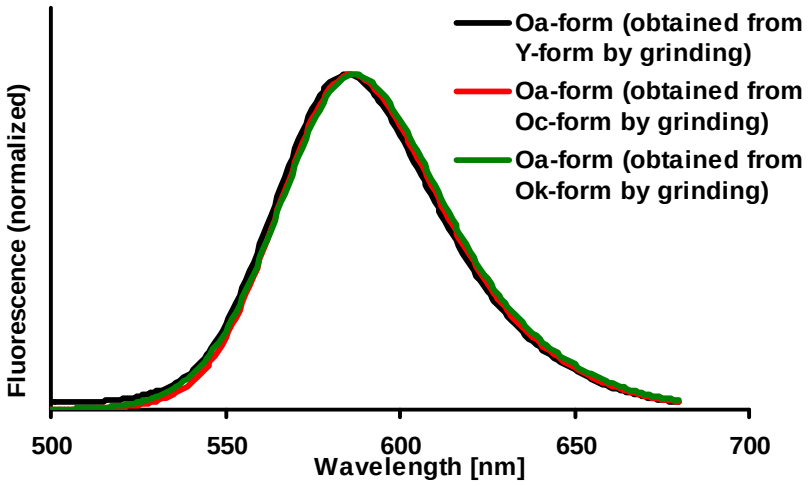

**9. Fluorescence life time**

Fluorescence decays were measured using an apparatus including a femtosecond laser system and a streak camera.[S2] The tetra(trimethylsilylethynyl)pyrene (**1**) was excited using by the SHG light of a femtosecond Ti:Sapphire laser (Spectra-Physics, Tsunami 3960, the wavelength of pulse ~ 800 nm, the full width at half maximum of the pulse ~80 fs) pumped by the SHG output of a Nd:$YVO_4$ laser (Spectra-Physics, Millennia-V). The detected fluorescence was dispersed by a monochromator and measured using a streak scope (Hamamatsu, C4334). The fluorescence signals were averaged using a PC. Fluorescence decay measurements were performed at 22 ºC for **1**. The fluorescence decay curve for each form of **1** can be represented by a single exponential decay function, $I(t)=I_o \exp(-t/\tau)$ where $\tau$ is the fluorescence lifetime.

**Figure S28.** Fluorescence decay profiles of **1**

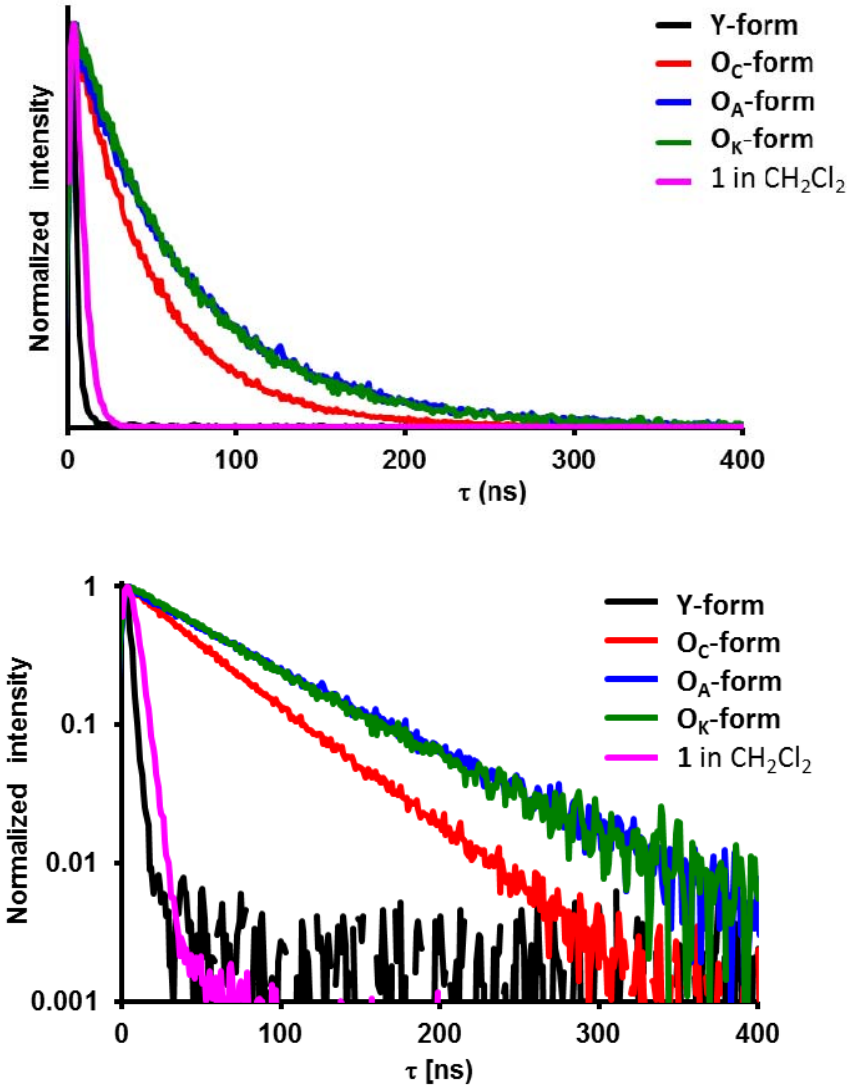

**Table S5.** Summary of emission lifetime, PL quantum yield and rate constants

| | **Y-form** | **$O_A$-form** | **$O_C$-form** | **$O_K$-form** | In $CH_2Cl_2$ |
|---|---|---|---|---|---|
| $\tau$ (ns) | 2.24 | 70.8 | 48.6 | 66.8 | 3.56 |
| $\Phi_F$ | 0.66 | 0.57 | 0.49 | 0.17 | --- |
| $k_r/k_{nr}$ ($\times 10^6$ $s^{-1}$) | 300/155 | 8.1/6.1 | 10.1/10.5 | 2.6/12.4 | --- |

The rate constants $k_r$ and $k_{nr}$ were calculated by using the following equations.

$$k_r = \Phi_F/\tau, \qquad k_{nr} = (1-\Phi_F)/\tau$$

**10. Thermogravimetry analysis (TGA)**

**Figure S29.** TGA thermogram of **$O_C$-form**

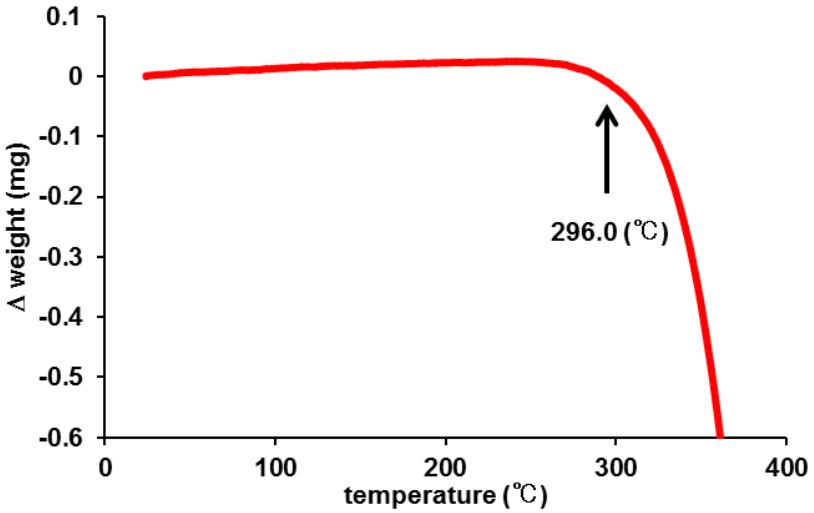


**11. UV—Vis and PL spectra of 1 in $CH_2Cl_2$**

**Figure S30.** UV—Vis absorption spectra of **1** in $CH_2Cl_2$ ($10^{-4}$ to $10^{-5}$ mol/L)

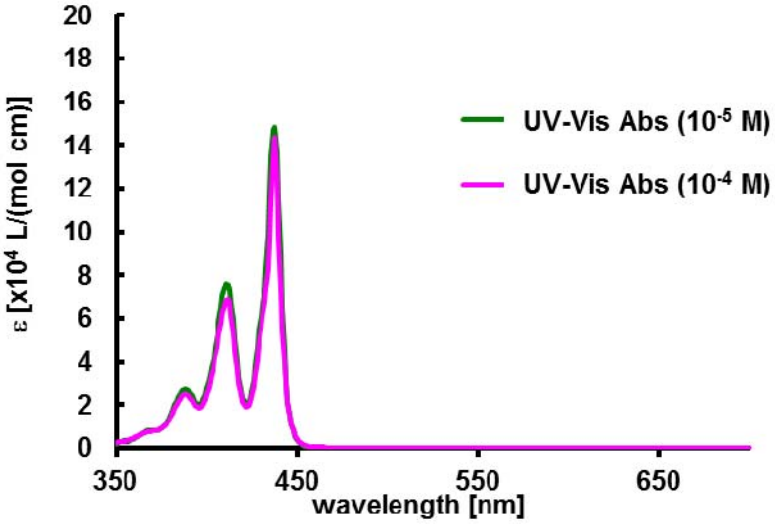

**Figure S31.** PL spectra of **1** in $CH_2Cl_2$ ($10^{-2}$ to $10^{-5}$ mol/L)

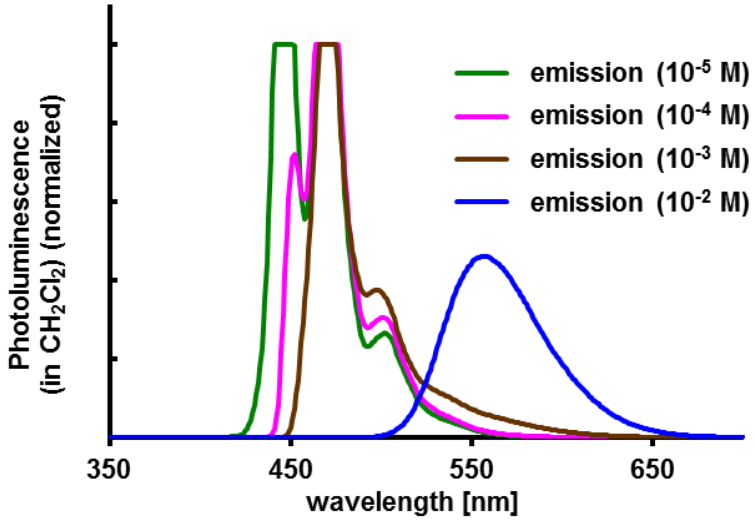


## 12. Microscopic observations of $O_C$-form on heating

**Figure S32.** Microscopic observations of **$O_C$-form** on heating

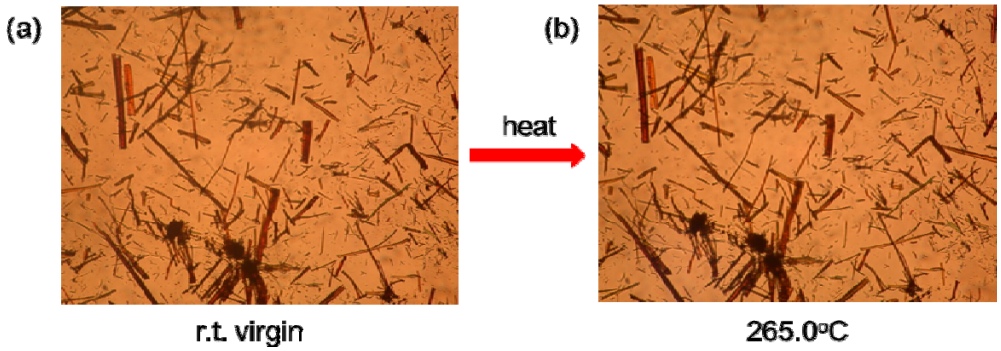


(a) orange needles of **$O_C$-form** which were obtained by reprecipitation from hexane
(b) orange needles of **$O_C$-form** which were heated at 265 °C

The microscopic observations showed no change of orange needles of the **$O_C$-form** on heating up to 265 °C.

**13. XRD analyses and microscopic observations of $O_K$-form on heating**

**Figure S33**. XRD profiles of **$O_K$-form** on heating

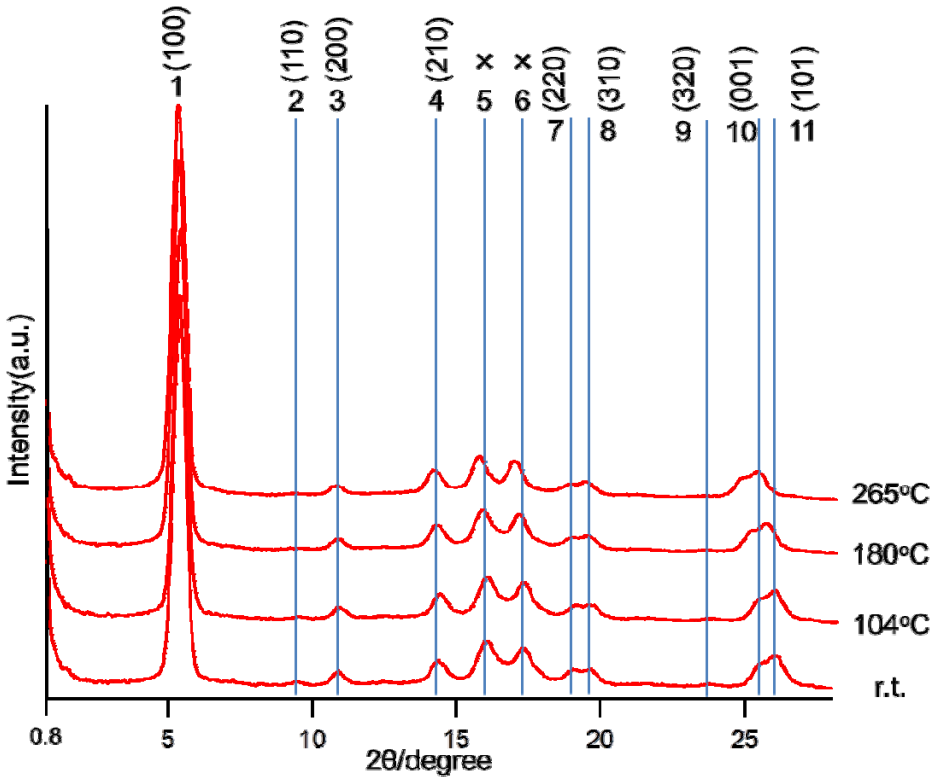


When the **OK-form** was heated, XRD analyses demonstrated that the peaks no. 5,6,10 and 11 were shifted to the lower angle region.

**Figure S34**. Microscopic observations of **$O_K$-form** on heating

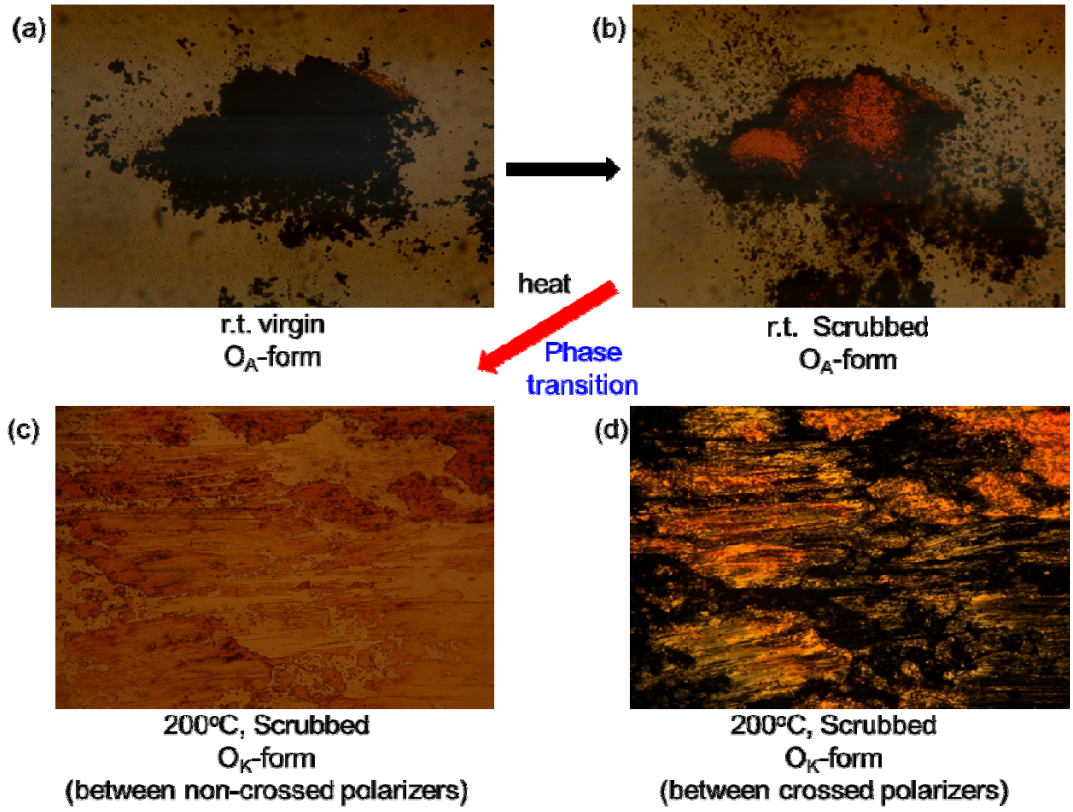


(a) **$O_A$-form** at rt
(b) **$O_A$-form** scrubbed between the cover glasses at rt

On heating, the **$O_A$-form** underwent a phase transition to **$O_K$-form**.
(c) **$O_K$-form** scrubbed between the cover glasses at 200 °C (between non-crossed polarizers)
(d) **$O_K$-form** scrubbed between the cover glasses at 200 °C (between crossed polarizers)

**$O_K$-form** was softer than **$O_A$-form**, and **$O_K$-form** was expanded between the glasses by scrubbing.

**14. References of Supporting Information and NMR charts of 1**

S1) H. Maeda, T. Maeda, K. Mizuno, K. Fujimoto, H. Shimizu, M. Inouye, *Chem. Eur. J.* 2006, **12**, 824.
S2) M. Takezaki, T. Tominaga, *J. Photochem. Photobiol. A*, 2005, **174**, 113.

Figure S35. NMR charts of 1 (CDCl3)

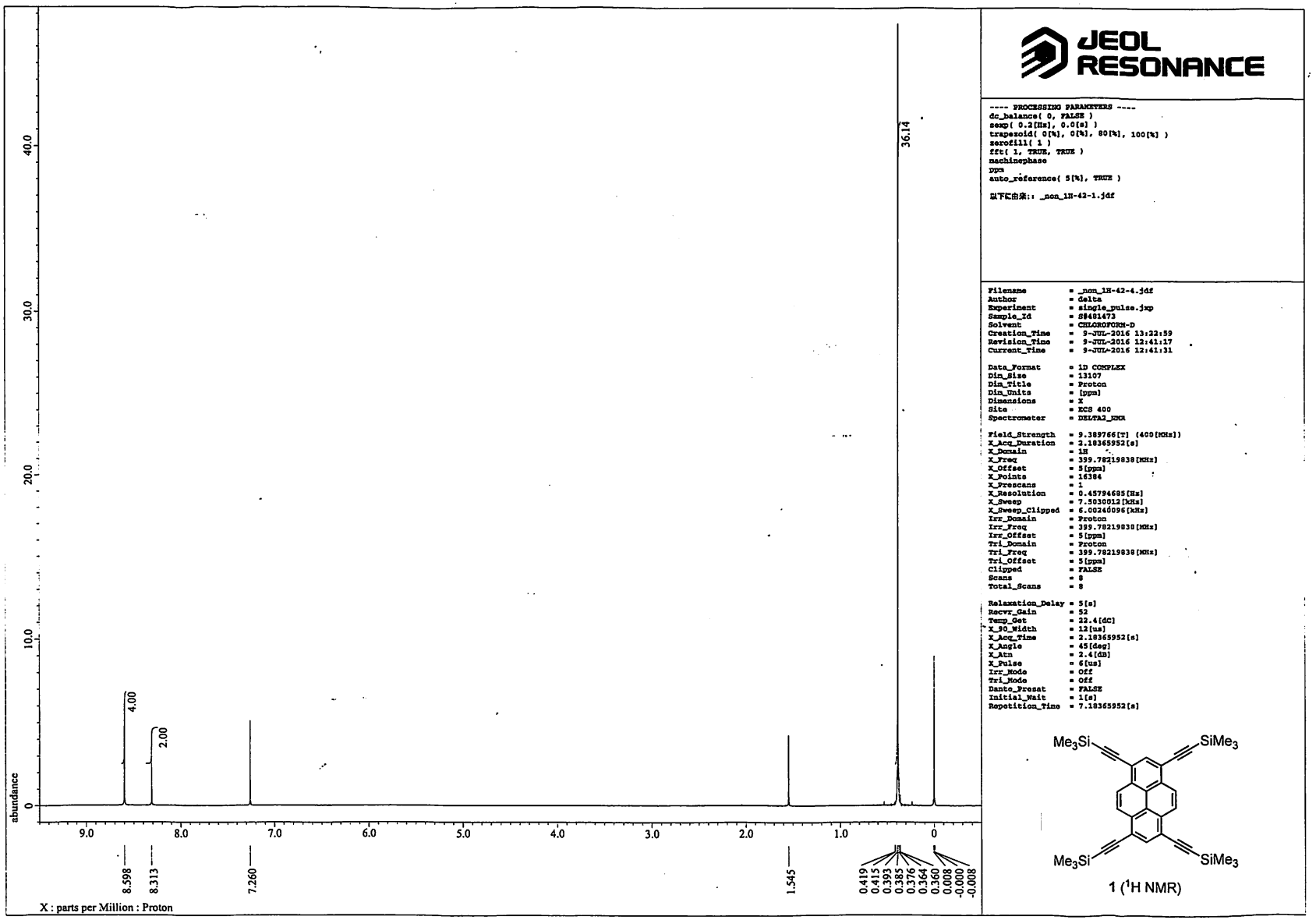

Figure S35. NMR charts of 1 (CDCl3)